Available online at www.sciencedirect.com
ScienceDirect
Journal of the European Ceramic Society 28 (2008) 2955–2962
www.elsevier.com/locate/jeurceramsoc

Fabrication and photoactivities of spherical-shaped $BiVO_4$ photocatalysts through solution combustion synthesis method

Hai-qing Jiang *, Hiromitsu Endo, Hirotaka Natori, Masayuki Nagai, Koichi Kobayashi

Research Center for Energy and Environmental Science, Advance Research Laboratories, Musashi Institute of Technology, Tokyo 158-0082, Japan

Received 22 February 2008; received in revised form 2 May 2008; accepted 9 May 2008
Available online 24 June 2008

Abstract

Spherical-shaped $BiVO_4$ photocatalysts were prepared by the solution combustion synthesis method. The as-prepared photocatalysts were characterized by X-ray diffraction (XRD), nitrogen absorption for the BET specific surface area, field emission scanning electron microscopy (FE-SEM) and ultraviolet–visible diffraction reflection spectroscopy (UV–vis). The $BiVO_4$ crystallites show a monoclinic structure with diameter of about 400–600 nm. UV–vis diffusion absorption spectra indicate that the band gap absorption edge of pure $BiVO_4$ crystallites prepared by the SCS method and the SSR method are 523 nm and 540 nm, corresponding to the band gap energies of 2.45 eV and 2.40 eV, respectively. It is also found that the photocatalytic activity of degradation of methylene blue improves when the molar ratio of fuels to oxidizer is 5.

Keywords: Powders-chemical preparation; Microstructure-final; Spectroscopy; Functional applications; $BiVO_4$

1. Introduction

Bismuth vanadate ($BiVO_4$) has attracted significant recent attention because of its good ferroelasticity,[1,2] ionic conductivity,[3] and its photocatalytic activity for degradation of organic materials[4] and organic dyes,[5–7] as well as for splitting of water for hydrogen[8] and oxygen evolution.[9,10] It is known that photocatalytic properties strongly depend on the crystal structure. $BiVO_4$ powder with a monoclinic structure shows high photocatalytic activity because of its relatively narrow band gap of 2.4 eV, as compared to $BiVO_4$ with a tetragonal phase (3.1 eV). Recently, various techniques are used to synthesize monoclinic structure $BiVO_4$ crystallites, such as aqueous process,[4,9,10] hydrothermal process,[5,6] sonochemical method,[7] organic decomposition method,[8] chemical bath deposition,[11] and solid-state reaction (SSR) method.[12]

In the present study, a solution combustion synthesis (SCS) method was used to prepare the $BiVO_4$ crystallites. The SCS method[13] has emerged as an important technique for the synthesis and processing of advanced ceramics, catalysts, composites, alloys, intermetallics and nanocrystallites. In particular, the SCS method of preparing oxide materials is a fairly recent development, and this technique has been used to produce homogeneous and fine crystalline powders.[14] The SCS method takes advantage of exothermic, fast and self-sustaining chemical reactions between metal salts and a suitable organic fuel, such as citric acid, urea, hydrazides, malonic acid dihydrazide, tetra formal tris azine, etc. Since most of the heat required for the synthesis is supplied by the reaction itself, the mixture of the reactants only needs to be heated to temperature that is significantly lower than the actual phase formation temperature. The energy expense involved is therefore limited.

2. Experimental procedure

2.1. Preparation of $BiVO_4$ crystallites

While previous attempts to fabricate $BiVO_4$ crystallites were carried out using citric acid or urea as fuels, we chose citric acid and urea as co-fuels. The experimental procedure for preparing $BiVO_4$ crystallites by the SCS method is schematically shown in Fig. 1. First, $Bi(NO_3)_3{\cdot}5H_2O$ (Wako, Japan) and the same molar quantity of citric acid (Wako, Japan) were dissolved in a nitric acid aqueous solution (Wako, Japan). After magnetic stirring for 30 min, a transparent solution was formed. $NH_3{\cdot}H_2O$ (Shawo, Japan) was then added to this solution to adjust the pH

* Corresponding author. Tel.: +81 3 57063259; fax: +81 3 57063259.
E-mail address: hgjiang@sc.musashi-tech.ac.jp (H.-q. Jiang).

0955-2219/$ – see front matter © 2008 Elsevier Ltd. All rights reserved.
doi:10.1016/j.jeurceramsoc.2008.05.002

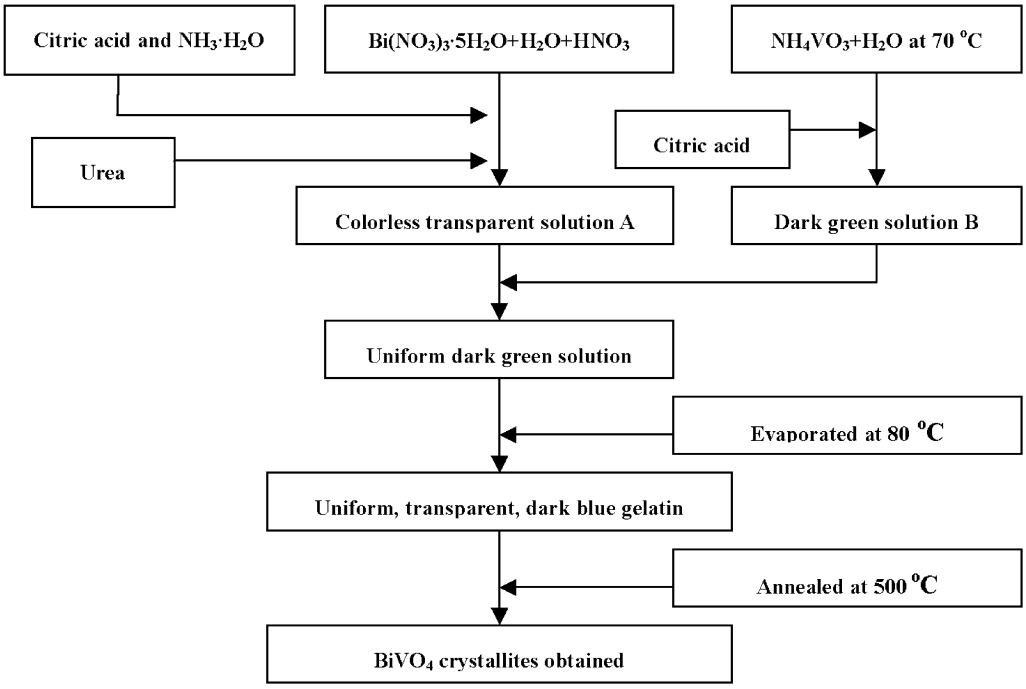

Fig. 1. Schematic diagram for the preparation of $BiVO_4$ using the solution combustion synthesis method.

value to 7.5. Finally, urea (Wako, Japan) was added to obtain a transparent solution A. Meanwhile, NH_4VO_3 (Wako, Japan) was dissolved in deionized water at 70 °C. The same molar quantity of citric acid was added to obtain a dark green solution B. After mixing solutions A and B, a uniform dark green solution was obtained. The mixture thus obtained was evaporated at 80 °C in a drying oven for 20 h. Finally, a transparent, uniform, deep blue gelatin is obtained. The $BiVO_4$ crystallites were synthesized by annealing the obtained gelatins at 480–500 °C in air for different times with a heating rate of 2 °C/min from room temperature to 300 °C and 3 °C/min from 300 °C to the annealing temperature.

In the process of preparing the gel, citric acid was not only employed as a fuel, but was also applied as a chelating agent. Urea was also used as a fuel at the same time, and it partially decomposed to ammonia and water to maintain the constancy of the pH value of the solution during the evaporation process. Ammonia solution was used to adjust pH value to 7.5. Simultaneously, ammonia solution reacted with the HNO_3 solution to form ammonium nitrate, which could be used as an oxidizer. According to the method proposed by Jain et al.[15] it is possible to calculate the elemental stoichiometric coefficient φ as the ratio between the total valence of the fuel (citric acid and urea) and the total valence of the oxidizers ($Bi(NO_3)_3{\cdot}5H_2O$, NH_4VO_3 and NH_4NO_3) according to Eq. (1):

$$\varphi = \frac{n[6\times(+4)_{(C)} + 8\times(+1)_{(H)} + 7\times(-2)_{(O)}] + m[(+4)_{(C)} + (-2)_{(O)} + 2\times 0_{(N)} + 2(+1)_{(H)}]}{x[3_{(Bi)} + 3(0_{(N)} + 3\times(-2)_{(O)})] + y[(+5)_{(V)} + 0_{(N)} + 4\times 1_{(H)} + 3\times(-2)_{(O)}] + z[2\times 0_{(N)} + 4\times(+1)_{(H)} + 3\times(-2)_{(O)}]} \quad (1)$$

Here, n, m, x, y and z represent the moles of citric acid, urea, $Bi(NO_3)_3{\cdot}5H_2O$, NH_4VO_3 and NH_4NO_3 (in this experiment, the theoretical amount of NH_4NO_3 is estimated equal to the amount of HNO_3, which is about 0.0236 mol), respectively. According to Eq. (1), $\varphi = 1$, $\varphi < 1$ and $\varphi > 1$ indicate the stoichiometric condition, an oxidant-rich condition and a fuel-rich condition, respectively. In our experiment, a series of $BiVO_4$ materials were prepared by the SCS method according to different elemental stoichiometric coefficients φ by adjusting the amount of urea (in this experiment, the amount of citric acid in each solution was kept constant).

In this experiment, the monoclinic structure $BiVO_4$ powders were also prepared through the solid-state reaction (SSR) method by mixing stoichiometric amounts of Bi_2O_3 (Osaka, Japan) and NH_4VO_3 (Wako, Japan). The mixed powders were firstly calcined at 700 °C for 20 h. Then the obtained powders were crushed by a mortar. Finally, the monoclinic structure $BiVO_4$ crystallites were synthesized at 900 °C for 10 h.

2.2. Characterizations

The wet gel precursor was characterized by TG–DTA (SII, Seiko instrument, Japan) at a heating rate of 15 °C/min under 150 cm^3/min flowing air condition. The phase structure of the as-prepared crystallites was investigated through X-ray diffraction (Cu Kα, Rint 2000, Ragaku. Co. Ltd., Japan). The diffusion reflection spectra of the as-prepared crystallites were recorded using a UV–vis spectrophotometer (UV-3100, Shimadzu Corporation, Japan). The specific surface area of $BiVO_4$ was measured through nitrogen adsorption BET method (Autosorb-1, Quantachrome Instruments, USA). The morphology was observed by

a field emission scanning electron microscope (S-4100, Hitachi Ltd., Japan).

The photocatalytic activities of the samples were evaluated by methylene blue degradation. A 500-W Xe lamp was used as the light source, and the irradiation power was adjusted to 20 mW cm^{-2} through an optometer (P9710, Gigahertz Optik, Germany). First, 5 mg sample was added to the 100 ml of 2 mmol dm^{-3} methylene blue solution. After ultrasonic treatment for 20 min, the solution was stirred for 12 h to reach adsorption–desorption equilibrium. The photocatalytic activity was measured in the range of 320–800 nm by using an optical glass filter. The temperature of the methylene blue solution stirred in a 100 ml beaker was about 25 °C. Samples were taken at 20 min intervals and separated by centrifugation. The absorbance of methylene blue was measured by the aforementioned UV–vis spectrophotometer.

3. Results and discussion

3.1. DTA–TG analysis of the precursor gel

Fig. 2 shows the typical thermal behavior of the precursor gel. The DTA curve indicates that there are two endothermic peaks and three exothermic peaks up to 500 °C. The broad endothermic peaks from 100 °C to 148 °C are attributed to the gradual evaporation of free water and absorbed water. The broad endothermic peak from 200 °C to 270 °C is due to the decomposition of different nitrates and ammonium nitrate, accompanied by significant weight loss. The sharply exothermic peak at 152 °C with dramatic weight loss in the TG curve is assigned to the decomposition of urea because the decomposition reaction of urea is exothermic reaction. The sharply exothermic peak at 283 °C corresponds to the decomposition and combustion of citrates. The small broad exothermic peak centered at 481 °C is due to the complete oxidation of residual carbon in the sample accompanied by approximate 3% weight loss. At the same time, a monoclinic phase structure $BiVO_4$ crystallites form at this temperature.

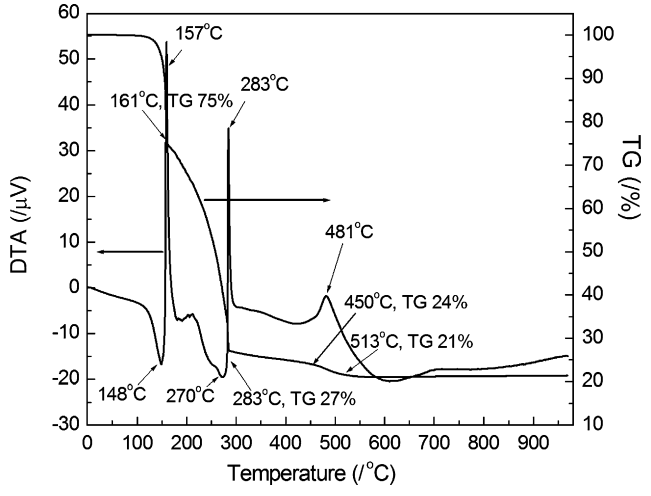

Fig. 2. DTA–TG curves of the $BiVO_4$ precursor gel.

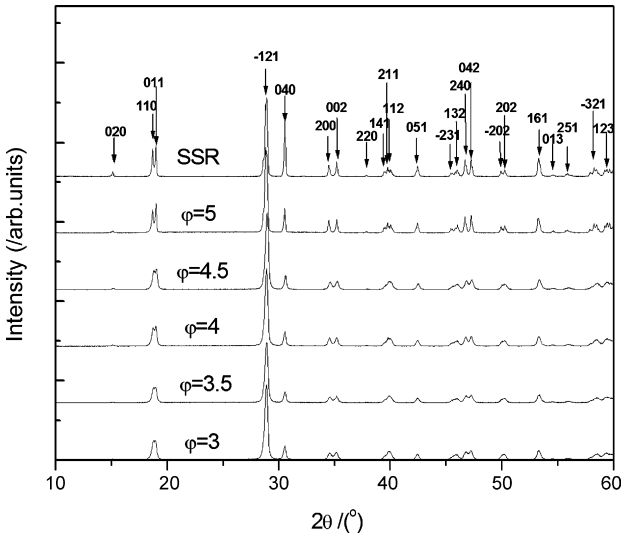

Fig. 3. XRD results for the $BiVO_4$ crystallites prepared by the SCS method with different values of φ (@ 500 °C, 4 h, in air) and by the SSR method (@ 900 °C. 10 h, in air).

3.2. XRD analysis

The XRD pattern (Fig. 3) shows that all the $BiVO_4$ crystallites have a monoclinic structure (JSPD file no. 14-688, space group: $I2/a$, $a = 5.195$, $b = 11.701$, $c = 5.092$, $\beta = 90.38$). Multi-peak separation fitting of samples prepared by the SCS method is carried out from 28° to 30° according to $\bar{1}$ 3 0, $\bar{1}$ 2 1 and 1 2 1 diffractive peaks. The results are shown in Fig. 4 and Table 1. It is obvious that the intensity of the diffractive peaks increases with the value of φ, indicating an increase in the degree of crystallinity. According to the multi-peaks separation results shown in Table 1, the intensity of the $\bar{1}$ 2 1 diffractive peak increases in comparison with $\bar{1}$ 3 0 and 1 2 1 diffractive peaks, which indicates the growth of $BiVO_4$ crystallites along the $\bar{1}$ 2 1 direction. The Scherer equation is used to calculate the particle sizes according to the FWHM of $\bar{1}$ 2 1 diffractive peak. The results indicate that the particle sizes along the $\bar{1}$ 2 1 direction increase with the increase of φ.

3.3. Characterization of morphology

The morphologies of the $BiVO_4$ crystallites are shown in Fig. 5. All the samples prepared by the SCS method are spherical-shape. The size of $BiVO_4$ crystallites is about

Table 1
XRD multi-peaks separation results of the $\bar{1}$ 2 1 peak for the $BiVO_4$ crystallites

φ	2θ (°)	d-Value	FWHM (°)	Intensity	Crystal size[a] (nm)
3	28.85	3.092	0.21	3,538	42
3.5	28.88	3.089	0.21	3,912	40
4	28.85	3.083	0.18	6,626	54
4.5	28.86	3.091	0.18	7,426	54
5	28.81	3.097	0.13	12,816	87

[a] Calculated according to the $\bar{1}$ 2 1 diffractive peak.

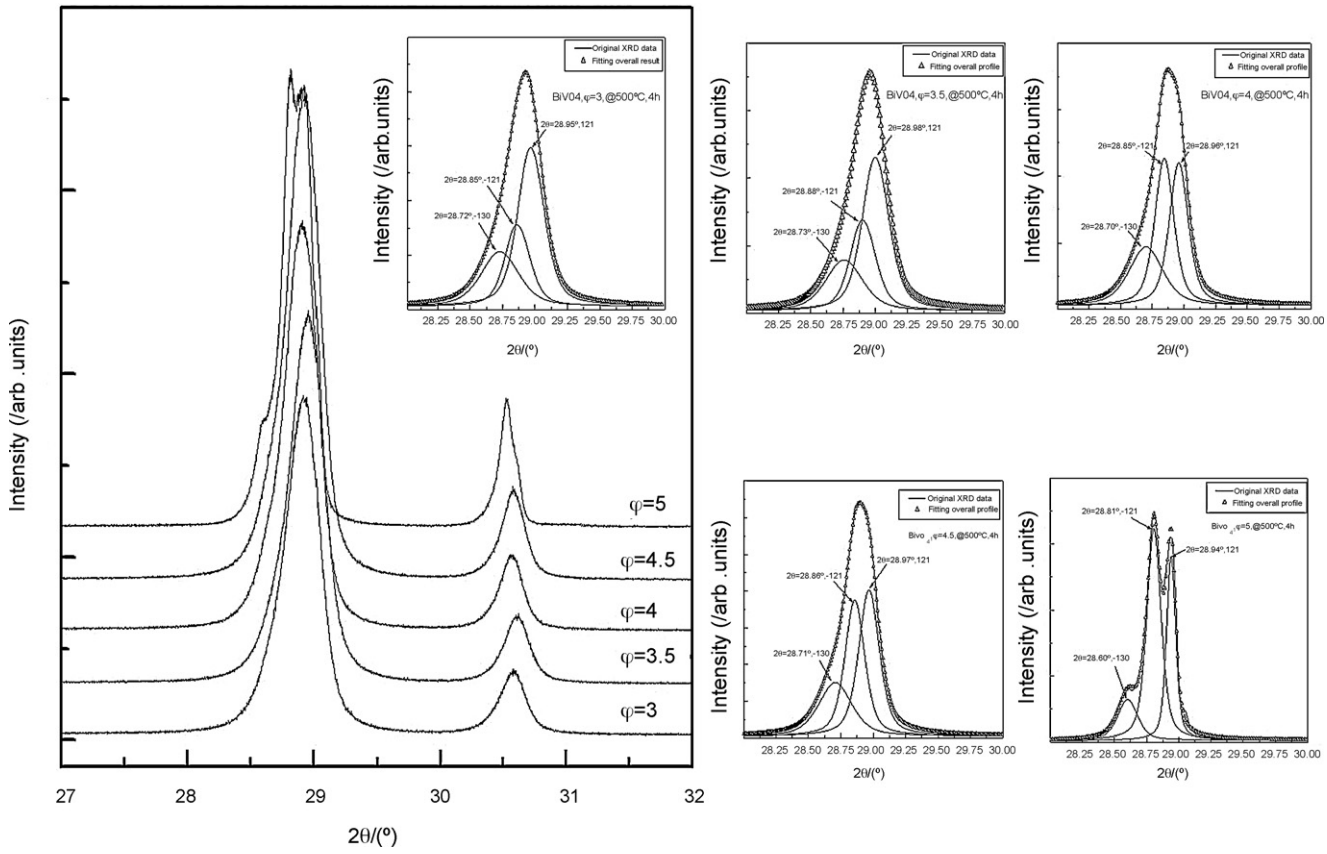

Fig. 4. XRD multi-peaks separation for the $BiVO_4$ crystallites prepared by the SCS method from 28° to 30° according to the $\bar{1}\,3\,0$, $\bar{1}\,2\,1$ and $1\,2\,1$ peaks.

400–600 nm. However, $BiVO_4$ crystallites prepared by SSR method exhibit irregular morphology with particle size about 1.5 μm.

In the process of the solution combustion technique, it is a significant step to prepare a semi-rigid gelatin with atomic level homogeneity. At pH 7.5, citric acid metal–chelate complexes are formed. During the evaporation of the solvent, the citric acid metal–chelate polymerize to promote uniformity of different metal ions, which can be achieved by encircling stable metal–chelate complexes in a growing polymer net. The randomness of the initial solution will be retained in the final polymeric gelatin because the gelatin consists of many chains twist and tangle together, wherein both cations and solvents are entrapped by steric hindrance. Immobilization of the metal–chelate complexes in such a semi-rigid organic polymer net can reduce segregation of specific metal ions during the decomposition process of the polymer at high temperatures. According to model proposed by Kakihana,[16] with the gradual increase of temperature, a group of polymer long chains break down and change to short polymer chains. Then, short polymer chains twist and tangle together to form spherical aggregated polymer particles. Finally, amounts of short polymer chains form fine crystallites after the polymer chains completely oxidized. At the same time, spherical aggregated polymer particles form the spherical aggregated $BiVO_4$ crystallites. As a consequence, fine crystallites retain on the surface of $BiVO_4$ crystallites and form a rough surface.

In Fig. 5, the sample with $\varphi = 5$ has a relatively smooth surface. In the SCS method, the maximum temperature of the combustion reaction depends on fuels and the amounts of fuels in the combustion reaction.[14] With the increase of amounts of fuels, the maximum of temperature increased. The sample with $\varphi = 5$ can reach to relatively high temperature during the annealing process, which can promote the growth of $BiVO_4$ crystallites and decrease the roughness of surface.

It can also be observed that all the samples prepared by the SCS method have a similar aggregate particle size, which is unrelated to the φ value, temperature or annealing time. It is our understanding that the aggregate particle size is dependent on the concentration of citric acid in the solution during the evaporation of the solution and the decomposition of the polymerized metal–citrate long chains. At low temperatures, the long chain metal–citrate polymer break down to short chains and aggregate together to form the aggregated polymer particles, which means that the aggregate particle size is decided at a relatively low temperature.

3.4. BET specific surface area

Table 2 shows the *s*pecific surface area of $BiVO_4$ measured by nitrogen adsorption BET method. The BET results indicate that the specific surface area of $BiVO_4$ crystallites increases slightly with the φ value when the φ value is less than 4. When the φ value is more than 4, the specific surface area of $BiVO_4$

crystallites gradually decrease with the φ value. At $\varphi = 5$, BET specific surface area of $BiVO_4$ crystallites is 1.76 $m^2\ g^{-1}$, which is about 2.4 times than that of $BiVO_4$ crystallites prepared by the SSR method.

3.5. UV–vis diffusion reflectance spectra

The color of the $BiVO_4$ crystallites is vivid yellow. Fig. 6 shows the UV–vis diffuse reflection spectra (DRS) of the $BiVO_4$

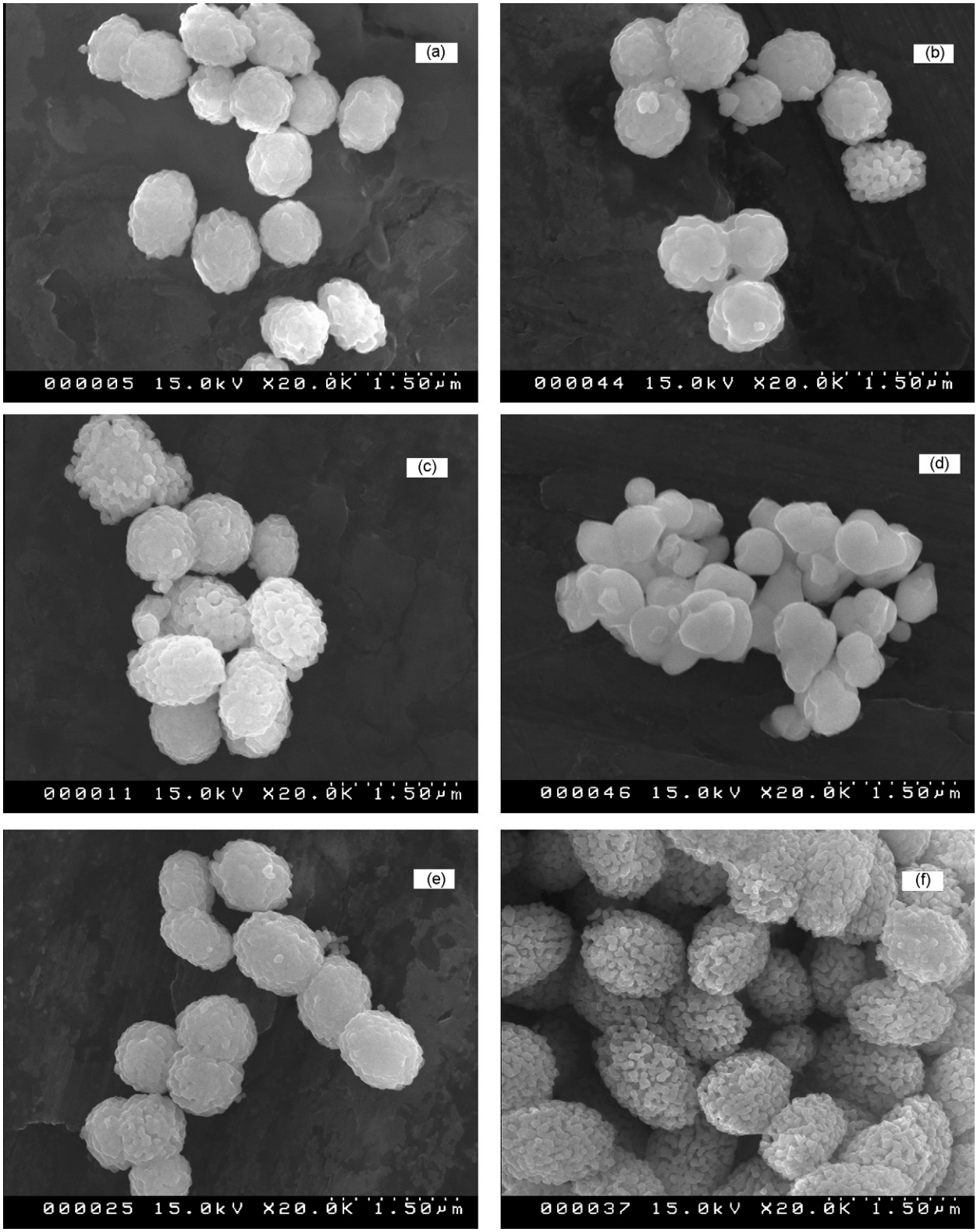

Fig. 5. FE-SEM micrograph of the $BiVO_4$ crystallites: (a) $\varphi = 3$, 500 °C, 4 h; (b) $\varphi = 4$, 500 °C, 4 h; (c) $\varphi = 4.5$, 500 °C, 4 h; (d) $\varphi = 5$, 500 °C, 4 h; (e) $\varphi = 3.5$, 500 °C, 1 h; (f) $\varphi = 3.5$, 500 °C, 0.2 h; (g) $\varphi = 3.5$, 490 °C, 1 h; (h) $\varphi = 3.5$, 510 °C, 1 h; (i) SSR, 900 °C, 10 h.

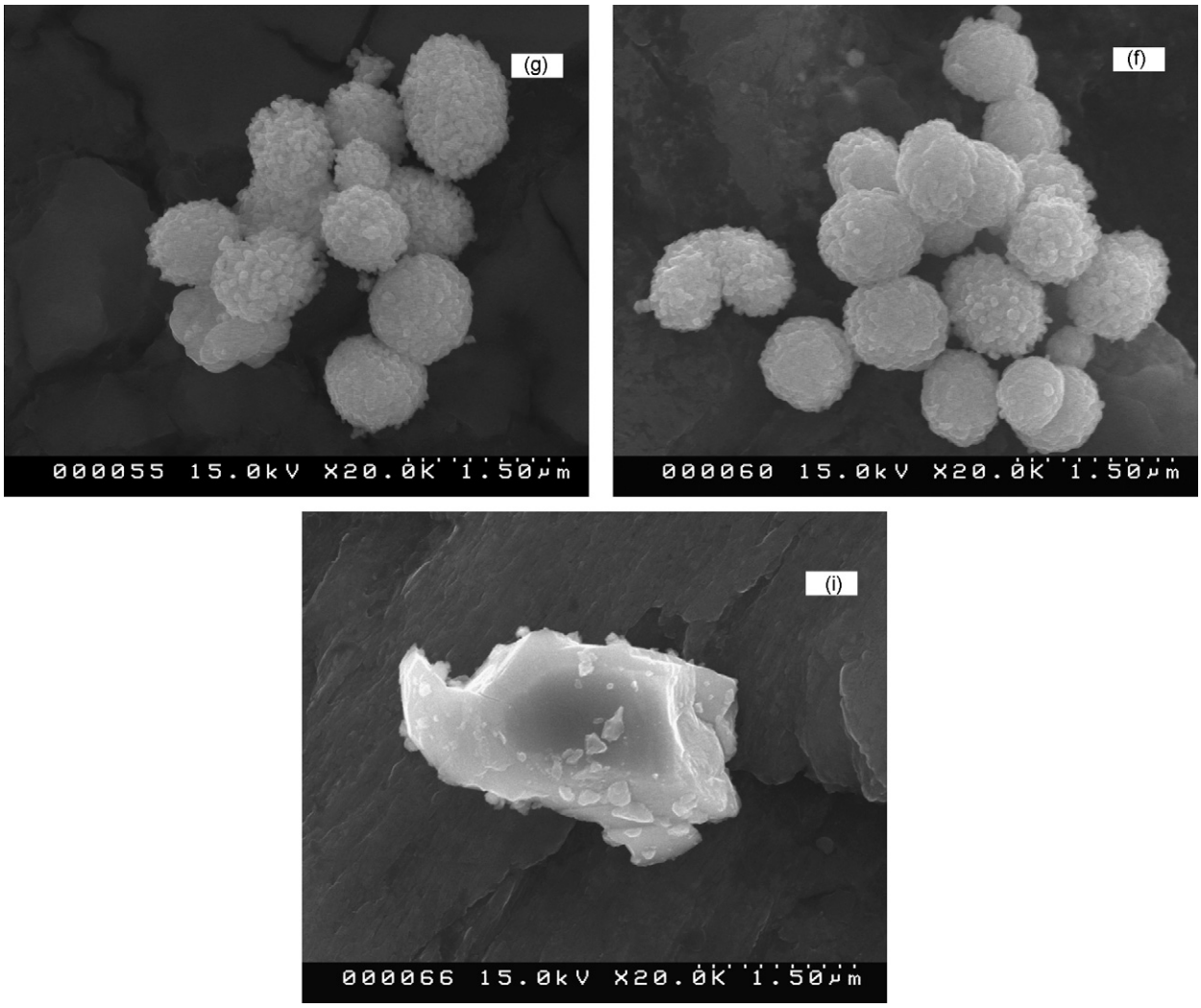

Fig. 5. (*Continued*).

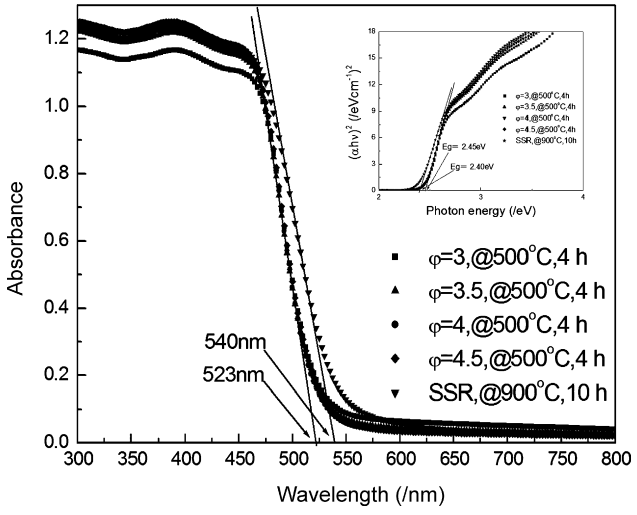

Fig. 6. UV–vis diffusion reflectance spectra of the $BiVO_4$ crystallites. The inset shows the relationship between $(\alpha h\nu)^2$ and the photon energy.

crystallites. The relationship between absorbance and incident photon energy $h\nu$ is described in Eq. (2) for direct electron transition:

$$(\alpha h\nu) = A(h\nu - E_g)^{1/2} \quad (2)$$

where A, E_g and $h\nu$ represent a constant, direct band gap energy and incident photon energy, respectively. The band gap absorption edges of the $BiVO_4$ crystallites prepared by the SCS method and the SSR method are determined to be 523 nm and 540 nm, corresponding to the band gap energies of 2.45 eV and 2.40 eV (shown in the inset in Fig. 6), respectively, which are

Table 2
BET specific surface area of $BiVO_4$ crystallites

Sample	BET specific surface area ($m^2\ g^{-1}$)
$\varphi = 3$	2.36
$\varphi = 3.5$	2.49
$\varphi = 4$	2.72
$\varphi = 4.5$	2.62
$\varphi = 5$	1.76
SSR	0.74

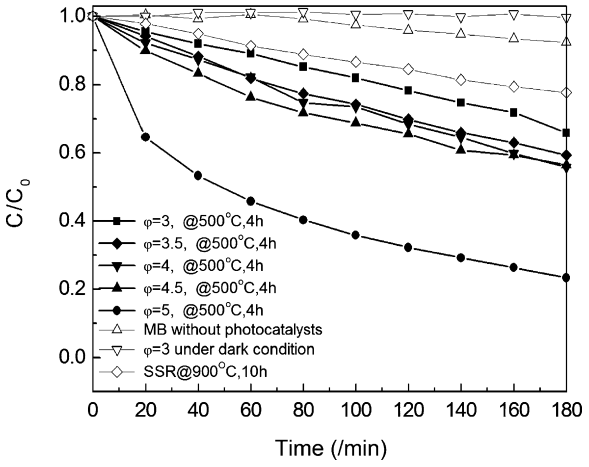

Fig. 7. Photocatalytic activity of $BiVO_4$ crystallites with different φ values.

the directly allowed optical transition. This is very consistent with the reported band gap value of the monoclinic $BiVO_4$.[9,10] The obvious blue shift of band gap absorption edges for $BiVO_4$ crystallites prepared by the SCS method comparing to the SSR method is observed, which is likely ascribed to quantum size effect caused by the difference of crystal size. According to the results of XRD and FE-SEM, the crystal size of $BiVO_4$ particles prepared by the SCS method is far less than that of $BiVO_4$ prepared by the SSR method. No obvious shift in the band gap absorption edge was observed among the samples prepared by the SCS method at the different φ values.

3.6. Photocatalytic activity for degradation of methylene blue solution

To determine the photocatalytic activity of the prepared $BiVO_4$ photocatalyst, an experiment was carried out using a methylene blue solution as the probe material with an initial concentration of 2 mmol dm^{-3}. The band edge position of the conduction band and the valance band of a semiconductor can be determined using a simple approach.[17,18] The conduction band edge of a semiconductor at the point of zero charge (pH_{ZPC}) can be predicted by Eq. (3):

$$E^0_{CB} = X - E^C - \frac{1}{2}E_g \quad (3)$$

Here, X is the absolute electronegativity of the semiconductor, expressed as the geometric mean of the absolute electronegativity of the constituent atoms, which is defined as the arithmetic mean of the atomic electron affinity and the first ionization energy (for $BiVO_4$, X is 6.035 eV[19]). E^C is the energy of free electrons on the hydrogen scale (~4.5 eV). E_g is the band gap of the semiconductor. According to Eq. (3), the positions of the conduction band and the valence band are 0.31 eV and 2.76 eV, respectively. After reaction with water, the holes photogenerated in the valence band can produce OH, O_2^-, H_2O_2 and O_2, which can effectively promote the degradation of the methylene blue solution.[20] The relation between C/C_0 and the reaction time is shown in Fig. 7. It is obvious that the photocatalytic activity of the samples increase with the increase of φ value. When the φ value is 5, the photocatalytic activity sharply increases, comparing to the other samples. From Fig. 5, it can be observed that the surface of the sample with $\varphi = 5$ is smooth without a rough morphology, which suggests an increase in the degree of crystallinity. The XRD results also reveal that the relative intensity of $\bar{1}\,2\,1$ diffractive peak of the sample with $\varphi = 5$ increases.

As a direct electron transition semiconductor, the monoclinic $BiVO_4$ crystal is excited by the incident photons with energy equal to or greater than their band energy level. The electrons receive energy from the photons and are thus promoted from the valence band to the conduction band, if the energy gained is higher than the band gap energy level. Electrons and holes that migrate to the surface of the semiconductor without recombination can respectively reduce or oxidize the reactants adsorbed by the semiconductor. In the process of migration to the surface of the semiconductor, the mobility of the photo-generated charge carriers is a key factor. If there are many crystal boundaries and defects in the semiconductor interior, which play the role of recombination centers for electrons and holes, this will hinder the diffusion of electrons and holes from the interior to the surface of the semiconductor. The photo-generated electrons and holes could recombine in the bulk or on the surface of the semi-

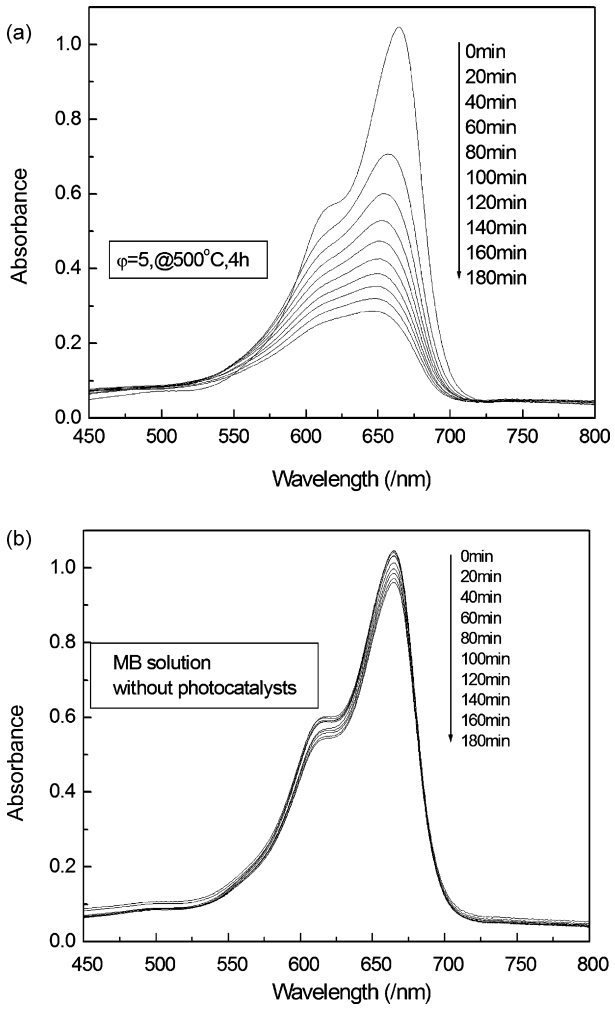

Fig. 8. Photodegradation process of methylene blue: (a) with $BiVO_4$ crystallites; (b) without $BiVO_4$ crystallites.

conductor within a very short time, releasing energy in the form of heat or photons. The photocatalytic activity decreases with fewer electrons and holes on the surface. For the sample with $\varphi = 5$, greater amounts of fuels can promote the degree of crystallinity and reduce the amounts of defects in the $BiVO_4$ crystal. Consequently, the photocatalytic activity increases. However, the sample prepared by the SSR method exhibits the worse photoactivities which can be ascribed to the increase of particle size, relatively low specific surface area and serious aggregation. Fig. 8 shows the photodegradation process of methylene blue over sample of $\varphi = 5$ and photolysis process of methylene blue without $BiVO_4$ photocatalysts.

4. Conclusions

Spherical and irregular shaped monoclinic $BiVO_4$ crystallites were prepared through the SCS method and the SSR method, respectively. The aggregate particle size of the $BiVO_4$ crystallites prepared by the SCS method is about 400–600 nm. The particle size of the $BiVO_4$ crystallites prepared by the SSR method is about 1.5 μm. With the increase of φ value, the degree of crystallinity of the $BiVO_4$ crystallites increases. When φ value is 5, the photocatalytic activity sharply increases. The value of C/C_0 is about 0.24 after 180 min and is about 3.5 times that of $BiVO_4$ prepared by the SSR method, which can be attributed to the increase in the crystallinity and a decrease in crystal defects. The band gap absorption edges of the $BiVO_4$ crystallites prepared by the SCS method and the SSR method are determined to be 523 nm and 540 nm, corresponding to the band gap energies of 2.45 eV and 2.40 eV, respectively.

References

1. Lim, A. R., Lee, K. H. and Choh, S. H., Domain wall of ferroelastic $BiVO_4$ studied by transmission electron microscopy. *Solid State Commun*, 1992, **83**, 185–186.
2. Hazen, R. M. and Mariathasan, J. W. E., Bismuth vanadate: a high-pressure, high-temperature crystallographic study of the ferroelastic–paraelastic transition. *Science*, 1982, **216**, 991–993.
3. Hirota, K., Komatsu, G., Yamashita, M., Takemura, H. and Yamaguchi, O., Formation, characterization and sintering of alkoxy-derived bismuth vanadate. *Mater Res Bull*, 1992, **2**, 823–830.
4. Xie, B. P., Zhang, H. X., Cai, P. X., Qiu, R. L. and Xiong, Y., Simultaneous photocatalytic reduction of Cr(VI) and oxidation of phenol over monoclinic $BiVO_4$ under visible light irradiation. *Chemosphere*, 2006, **63**, 956–963.
5. Zhang, X., Ai, Z. H., Jia, F. L., Zhang, L. Z., Fan, X. X. and Zou, Z. G., Selective synthesis and visible-light photocatalytic activities of $BiVO_4$ with different crystalline phases. *Mater Chem Phys*, 2007, **103**, 162–167.
6. Zhang, L., Chen, D. R. and Jiao, X. L., Monoclinic structured $BiVO_4$ nanosheets: hydrothermal preparation, formation mechanism, and coloristic and photocatalytic properties. *J Phys Chem B*, 2006, **110**, 2668–2673.
7. Zhou, L., Wang, W., Liu, S., Zhang, L., Xu, H. and Zhu, W., A sonochemical route to visible-light-driven high-activity $BiVO_4$ photocatalys. *J Mol Catal A Chem*, 2006, **252**, 120–124.
8. Sayama, K., Nomura, A., Arai, T., Sugita, T., Abe, R., Yanagida, M. *et al.*, Photoelectrochemical decomposition of water into H_2 and O_2 on porous $BiVO_4$ thin-film electrodes under visible light and significant effect of Ag ion treatment. *J Phys Chem B*, 2006, **110**, 11352–11360.
9. Kudo, A., Omori, K. and Kato, H., A novel aqueous process for preparation of crystal form-controlled and highly crystalline $BiVO_4$ powder from layered vanadates at room temperature and its photocatalytic and photophysical properties. *J Am Chem Soc*, 1999, **121**, 11459–11467.
10. Tokunaga, S., Kato, H. and Kudo, A., Selective preparation of monoclinic and tetragonal $BiVO_4$ with scheelite structure and their photocatalytic properties. *Chem Mater*, 2001, **13**, 4624–4628.
11. Neves, M. C. and Trindade, T., Chemical bath deposition of $BiVO_4$. *Thin Solid Films*, 2002, **406**, 93–97.
12. Sleight, A. W., Chen, H. Y., Ferretti, A. and Cox, D. E., Crystal growth and structure of $BiVO_4$. *Mater Res Bull*, 1979, **14**, 1571–1581.
13. Patila, K. C., Arunab, S. T. and Mimania, T., Combustion synthesis: an update. *Curr Opin Solid State Mater Sci*, 2002, **6**, 507–512.
14. Hwang, C. C., Wu, T. Y., Wan, J. and Tsai, J. S., Development of a novel combustion synthesis method for synthesizing of ceramic oxide powders. *Mater Sci Eng B*, 2004, **111**, 49–56.
15. Jain, S. R., Adiga, K. C. and Verneker, V. R. P., A new approach to thermochemical calculations of condensed fuel–oxidizer mixtures. *Combust Flame*, 1981, **40**, 71–79.
16. Kakihana, M., Invited review "Sol–Gel" Preparation of high temperature superconducting oxides. *J Sol Gel Sci Technol*, 1996, **6**, 7–55.
17. Butler, M. A. and Ginley, D. S., Prediction of flatband potentials at semiconductor-electrolyte interfaces from atomic electronegativities. *J Electrochem Soc*, 1978, **125**, 228–232.
18. Xu, Y. and Schoonen, M. A. A., The absolute energy positions of conduction and valence bands of selected semiconducting minerals. *Am Mineral*, 2000, **85**, 543–556.
19. Long, M. C., Cai, W. M., Cai, J., Zhou, B. X., Chai, X. Y. and Wu, Y. H., Efficient photocatalytic degradation of phenol over $Co_3O_4/BiVO_4$ composite under visible light irradiation. *J Phys Chem B*, 2006, **110**, 20211–20216.
20. Fujishima, A., Zhang, X. T. and Tryk, D. A., Heterogeneous photocatalysis: from water photolysis to applications in environmental cleanup. *Int J Hydrogen Energy*, 2007, **32**, 2664–2672.